JOURNAL OF GUIDANCE, CONTROL, AND DYNAMICS
Vol. 21, No. 1, January–February 1998

Long-Term Formation Keeping of Satellite Constellation Using Linear-Quadratic Controller

Yuri Ulybyshev
Rocket-Space Corporation "Energia," Korolev, Moscow Region 141070, Russia

Relative formation keeping of a satellite constellation in circular orbits is investigated. The in-plane formation keeping based on tangential maneuvers is defined with use of the averaged equations representing secular relative motion in a neighborhood of a circular reference orbit. The state variables are along-track displacements of satellites (without periodic terms) relative to prescribed intersatellite spacings and displacements of satellite orbital periods with respect to the reference orbit period. A set of along-track relative displacements between satellites is represented by a tree digraph. Long-term behavior of a satellite constellation is described by the linear discrete-time equation in terms of $(2N - 1)$ variables, where N is the total number of satellites. A new linear-quadratic controller for satellite constellations is developed. The formation keeping robustness is discussed. An analytic solution of linear-quadratic formation keeping for two satellites is obtained. Simulation results are presented for the low-altitude satellite constellation affected by atmospheric drag.

Nomenclature

$\boldsymbol{A}$	= state matrix
$\boldsymbol{A}_t$	= transposed incidence matrix of digraph
b, n, r	= out-of-plane, along-track, and radial relative position coordinates; Fig. 1
$\boldsymbol{F}, f$	= feedback matrix and its element
$\boldsymbol{G}, g$	= weighting matrix and its element
$\boldsymbol{I}$	= identity matrix
i	= satellite number
J	= cost function
j	= number of digraph edge
k	= sampling stage
N	= total number of satellites
$\boldsymbol{P}, p$	= Riccati equation (12) solution matrix and its element
$\boldsymbol{P}_n, \boldsymbol{P}_{nt}, \boldsymbol{P}_t$	= submatrices of matrix $\boldsymbol{P}$; Eq. (13)
R	= radius of circular reference orbit
T	= orbital period
t	= time
$\boldsymbol{v}, \Delta V_i$	= vector of tangential impulsive velocity changes and its element
$\boldsymbol{x}$	= state vector
$\Delta \boldsymbol{n}, \Delta n_i$	= vector of along-track displacements of satellites relative to idealized point on a circular reference orbit and its element
$\Delta \boldsymbol{T}, \Delta T_i$	= vector of orbital period displacements and its element
Δt	= time interval between maneuvers
$\delta \boldsymbol{n}, \delta n_j$	= vector of along-track relative displacements and its elements
λ	= closed-loop eigenvalue
ω	= mean motion of circular reference orbit
$\boldsymbol{0}$	= zero matrix or vector

I. Introduction

In recent years, with the emphasis on global communication, several satellite-based systems have been proposed based on multiple-satellite constellations in low Earth orbits.[1] The formation keeping of such large constellations poses new problems at the interface between the theory of orbital transfers and the control theory of large-scale systems. Similar formation keeping requirements are foreseen for the Earth observing system satellite missions, where two or more satellites must fly over the same point on the Earth with prescribed time spacing.

Formation keeping of a satellite constellation in circular orbits has been considered by Lamy and Pascal.[2] In Ref. 2 the state variables are phases of each satellite with respect to the mean satellite constellation. Glickman[3] developed a timed-destination approach to constellation formation keeping in which individual satellite flight path errors are indirectly controlled by closing control loops on timing and position errors in reaching a series of precomputed equatorial destinations. Calvet et al.[4] studied a simplified discrete-time linear model for describing dynamical behavior of the perturbed satellite constellation on a midterm interval. The optimal strategy has been defined using a two-level decomposition method based on linear programming and parametric optimization. A method of autonomous ring formation for a planar constellation of satellites based on the concept of potential functions was presented by McInnes.[5] An onboard formation keeping strategy has developed by Collins et al.[6]

Formation keeping of two satellites has been studied by several authors.[7–11] Another prototype of a simultaneous control of two or more satellites is the collocation problem for geostationary

Yuri Ulybyshev graduated from the Bauman Moscow High Technical School in Flight Dynamics and Control. Since 1977 he has worked in the Space Ballistics Department of NPO "Energia" (now Rocket-Space Corporation "Energia"). He has been involved in various space projects, such as the space shuttle Buran, the launch vehicle Energia, the spacecraft Soyz-T, the geostationary satellite Yamal, and others. In 1990 he received his Candidate of Technical Sciences Degree (Ph.D.) in Dynamics, Ballistics, and Automatic Control of Spacecrafts and Rockets. His research interests include astrodynamics, spacecraft design, and control theory. E-mail: yuri.ulybyshev@rsce.ru.

Received Nov. 8, 1994; revision received July 17, 1997; accepted for publication Aug. 21, 1997.

satellites.[12,13] The linear-quadratic formation keeping of two satellites has been studied by Vassar and Sherwood,[7] by Redding et al.,[9] and by Wilde et al.[13] In a sense, the work presented here extends the capabilities of linear-quadratic controllers to the formation keeping problem.[6,9,13]

We shall distinguish between relative and absolute formation keeping.[2,3,6] Relative formation keeping is maintaining the relative positions between satellites but not their absolute positions. In the case of absolute formation keeping, each satellite is maintained within a defined box moving with the idealized point on a reference orbit. This strategy can be effectively realized by simply closing the loop on the equatorial crossing time.[3] In this paper, a solution to relative formation keeping is presented.

The method to be described is based on the use of a tree digraph of the model satellite constellation. The goals are to show, first, that a classical linear-quadratic control theory can be useful in solving the difficult problem of simultaneous control of many satellites and, second, that this area can be a stimulus to new and interesting forms of large-scale control systems. The contribution of the paper is the demonstration that a feedback algorithm based on a linear-quadratic controller shows excellent performance and robustness and, hence, is a good candidate for satellite constellation formation keeping.

II. Mathematical Model

Relative Motion of Satellites in Circular Orbits

The Clohessy–Wiltshire equations[14] describe the motion of a satellite to a point on a circular reference orbit. They are

$$\ddot{n} = -2\omega\dot{r}, \qquad \ddot{r} = 3\omega^2 r + 2\omega\dot{n}, \qquad \ddot{b} = -\omega^2 b \tag{1}$$

where n, r, and b are coordinates in the orbit normal coordinate frame (Fig. 1).

It is well known that an approximate solution of the Clohessy–Wiltshire equations, when averaged from t to $t + 2\pi/\omega$ and ignoring the periodic terms, can be written as[8,10]

$$\dot{n}^* = -\frac{R\omega^2 \Delta T^*}{2\pi} \tag{2}$$

where ΔT^* is the displacement of the satellite orbital period relative to reference orbit period.

The following analysis is based on tangential maneuvers. The required tangential velocity change to kill the averaged (or secular) drift is[10]

$$\Delta V^* = \dot{n}^*/3 \tag{3}$$

We assume that the time interval between maneuvers is $\Delta t = \text{const}$ and introduce the following dimensionless variables in the following equations: $n = n^*/(R\omega\Delta t)$, $\Delta T = \Delta T^*/T = \omega\Delta T^*/2\pi$, and $\Delta V = 3\Delta V^*/(R\omega)$.

The prescribed positions of the satellites along their orbits can be represented by a set of constant phases about an idealized point (or a fictitious satellite) on a circular reference orbit. For the

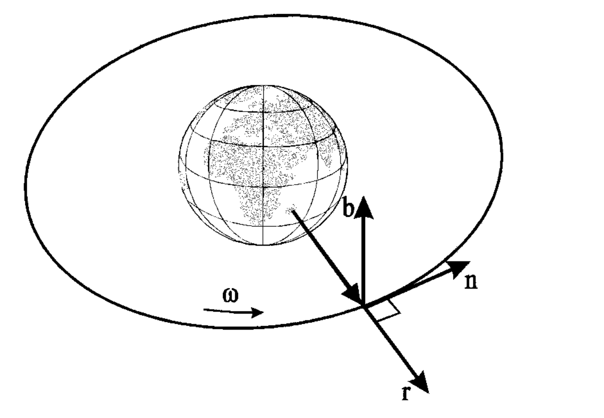

Fig. 1 Coordinate frame.

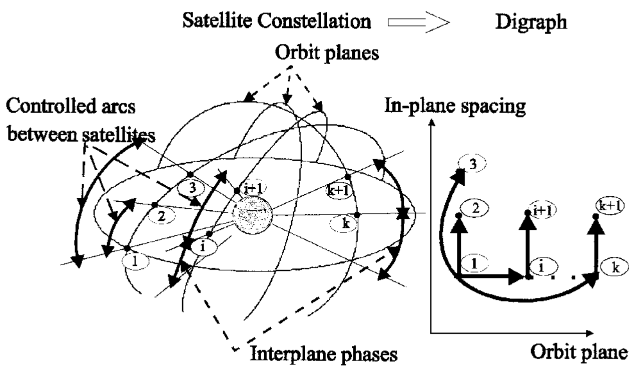

Fig. 2 Satellite constellation and its digraph: †, satellite and , number of satellite.

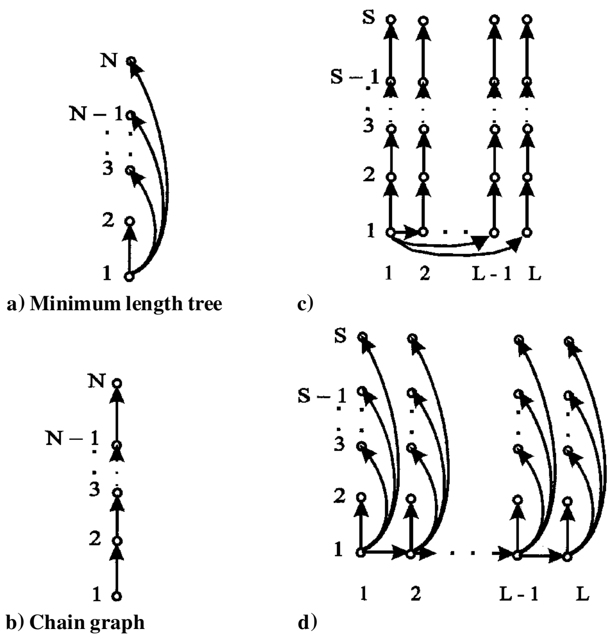

Fig. 3 Tree digraphs.

displacements relative to these phases, we can write N uncoupled discrete-time equations

$$\begin{Bmatrix} \Delta n_i(k+1) \\ \Delta T_i(k+1) \end{Bmatrix} = \begin{bmatrix} 1 & -1 \\ 0 & 1 \end{bmatrix} \begin{Bmatrix} \Delta n_i(k) \\ \Delta T_i(k) \end{Bmatrix} + \begin{bmatrix} 0 \\ 1 \end{bmatrix} \Delta V_i(k)$$
$$i = 1, \ldots, N \tag{4}$$

Discrete-Time Equation for Satellite Constellation

The prescribed intersatellite spacings of a satellite constellation can be represented by a digraph (Fig. 2). The satellites are the vertices. A link from one satellite to another is a directed edge or controlled arc between satellites. One of the satellites is taken as the first satellite and called the root of the digraph. The necessary conditions are weak connectedness of the digraph and the use of only simple paths. This digraph is a tree. Every tree with N vertices has precisely $N - 1$ edges.[15] Each digraph edge between two satellites is the prescribed along-track spacing. For two satellites in different orbit planes, it is the interplane phase. The along-track displacement δn_j is defined relative to this prescribed value, where j is the number of the edge. There are different variants of digraphs. Two digraph types may be cited as opposite variants. The first is the minimum length tree (MLT) (Fig. 3a) with equal length for all of the paths. The second is the digraph with maximum length equal to $N - 1$, i.e., the chain graph (CG) (Fig. 3b). Other variants can be represented as the geometry of the satellite constellation. For the satellite constellation with L orbit planes and S satellites in each orbit plane, examples of possible digraphs are shown in Figs. 3c and 3d. We used the following notations: for the MLT, $N \times 1$; for the CG, $1 \times N$; and for the other variants, $L \times S$ (Fig. 3c).

An incidence matrix associated with a digraph is an $N \times (N-1)$ matrix whose rows and columns correspond to the vertices and edges, respectively.[15] Coefficients of the incidence matrix consist of $-1, 0, 1$. The coefficient is zero if a vertex is not incident with an arc, $+1$ if the arc is oriented away from vertex, and -1 in the opposite case. The transposed incidence matrices $\boldsymbol{A}_t$ (with all of the unspecified elements equal to zero) for the MLT and the CG are given, respectively, as follows:

$$\boldsymbol{A}_t = \begin{bmatrix} 1 & -1 & & & & \\ 1 & & -1 & & & \\ 1 & & & -1 & & \\ . & . & . & . & . & . \\ 1 & & & & -1 & \\ 1 & & & & & -1 \end{bmatrix} \tag{5a}$$

$$\boldsymbol{A}_t = \begin{bmatrix} 1 & -1 & & & & \\ & 1 & -1 & & & \\ & & 1 & -1 & & \\ . & . & . & . & . & . \\ & & & 1 & -1 & \\ & & & & 1 & -1 \end{bmatrix} \tag{5b}$$

Next we introduce the state vector $\boldsymbol{x}^T = (\delta\boldsymbol{n}^T, \Delta\boldsymbol{T}^T) = (\delta n_1, \delta n_2, \ldots, \delta n_{N-1}, \Delta T_1, \Delta T_2, \ldots, \Delta T_N)$, where $\delta n_j = \Delta n_i - \Delta n_{i+1}$. There is a linear relation between $\Delta\boldsymbol{n}^T = (\Delta n_1, \Delta n_2, \ldots, \Delta n_N)$ and the along-track relative displacements:

$$\delta\boldsymbol{n} = \boldsymbol{A}_t \Delta\boldsymbol{n} \tag{6}$$

In summary, the state matrix can be written as

$$\boldsymbol{A} = \begin{bmatrix} \boldsymbol{I}_{N-1} & \boldsymbol{A}_t \\ \boldsymbol{0}_{(N-1)\times N} & \boldsymbol{I}_N \end{bmatrix} \tag{7}$$

where $\boldsymbol{I}_{N-1}$ and $\boldsymbol{I}_N$ are identity matrices and $\boldsymbol{0}_{(N-1)\times N}$ is a zero matrix. A long-term behavior for satellite constellation can be described by the multivariable discrete-time equation in a standard form

$$\boldsymbol{x}(k+1) = \boldsymbol{A}\boldsymbol{x}(k) + \boldsymbol{B}\boldsymbol{v}(k) \tag{8}$$

where $\boldsymbol{B}^T = [\boldsymbol{0}_{(N-1)\times N} \ \ \boldsymbol{I}_N]$ is a $(2N-1)\times N$ matrix and $\boldsymbol{v}^T = (\Delta V_1, \Delta V_2, \ldots, \Delta V_N)$ is the control vector. The system (8) is completely state controllable, where the rank of the controllability matrix[16] is $2N-1$. We hope that the represented mathematical model based on a tree digraph can be used in other applications.

III. Formation Keeping of Satellite Constellations

Linear-Quadratic Formation Keeping

The linear-quadratic formation keeping (LQF) may be as follows. Given the linear discrete-time equation (8), determine the optimal control law to minimize the following cost function:

$$J = \frac{1}{2}\sum_{k=0}^{k=k_f}\left[\boldsymbol{x}^T(k+1)\boldsymbol{G}_x\boldsymbol{x}(k+1) + \boldsymbol{v}^T(k)\boldsymbol{G}_V\boldsymbol{v}(k)\right] \tag{9}$$

where $\boldsymbol{G}_x$ is a positive definite or positive semidefinite matrix and $\boldsymbol{G}_v$ is a positive definite matrix. Matrices $\boldsymbol{G}_x$ and $\boldsymbol{G}_v$ are selected to weight the relative importance of the performance measures caused by the state vector $\boldsymbol{x}$ and control vector $\boldsymbol{v}$, respectively. These matrices can be diagonal with elements equal to the inverse square of the nominal deviation of the state variables and ΔV_i.

The optimal closed-loop control vector $\boldsymbol{v}(k)$ has the very well-known form[16]

$$\boldsymbol{v}(k) = -\boldsymbol{F}(k)\boldsymbol{x}(k) \qquad k = 0, 1, 2, \ldots, k_f \tag{10}$$

where $\boldsymbol{F}(k)$ is a $(2N-1)\times N$ feedback matrix:

$$\boldsymbol{F}(k) = \left[\boldsymbol{G}_V + \boldsymbol{B}^T\boldsymbol{P}(k+1)\boldsymbol{B}\right]^{-1}\boldsymbol{B}^T\boldsymbol{P}(k+1)\boldsymbol{A} \tag{11}$$

where $\boldsymbol{P}(k)$ is a positive solution of the Riccati equation[16]:

$$\boldsymbol{P}(k) = \boldsymbol{A}^T\boldsymbol{P}(k+1)\boldsymbol{A} - \boldsymbol{A}^T\boldsymbol{P}(k+1) \times \boldsymbol{B}\left[\boldsymbol{G}_V + \boldsymbol{B}^T\boldsymbol{P}(k+1)\boldsymbol{B}\right]^{-1}\boldsymbol{B}^T\boldsymbol{P}(k+1)\boldsymbol{A} + \boldsymbol{G}_X \tag{12}$$

with the terminal condition $\boldsymbol{P}(k_f) = 0$.

Suppose that $\boldsymbol{G}_X$ and $\boldsymbol{P}$ are

$$\boldsymbol{G}_x = \begin{bmatrix} \boldsymbol{G}_n & \boldsymbol{0} \\ \boldsymbol{0} & \boldsymbol{G}_t \end{bmatrix} \tag{13a}$$

$$\boldsymbol{P} = \begin{bmatrix} \boldsymbol{P}_n & \boldsymbol{P}_{nt} \\ \boldsymbol{P}_{nt}^T & \boldsymbol{P}_t \end{bmatrix} \tag{13b}$$

Referring to Eqs. (8) and (9), we obtain the state equations and J as follows:

$$\delta\boldsymbol{n}(k+1) = \delta\boldsymbol{n}(k) + \boldsymbol{A}_t\Delta\boldsymbol{T}(k) \tag{14}$$

$$\Delta\boldsymbol{T}(k+1) = \Delta\boldsymbol{T}(k) + \boldsymbol{v}(k) \tag{15}$$

$$J = \frac{1}{2}\sum_{k=0}^{k=k_f}\left[\delta\boldsymbol{n}^T(k+1)\boldsymbol{G}_n\delta\boldsymbol{n}(k+1) + \Delta\boldsymbol{T}^T(k+1)\boldsymbol{G}_t\Delta\boldsymbol{T}(k+1) + \boldsymbol{v}^T(k)\boldsymbol{G}_V\boldsymbol{v}(k)\right] \tag{16}$$

Substituting expressions (14–16) into Eqs. (11) and (12) yields the control law

$$\boldsymbol{v}(k) = -\boldsymbol{P}_S(k+1)\left\{\boldsymbol{P}_{nt}^T(k+1)\delta\boldsymbol{n} + \left[\boldsymbol{P}_{nt}^T(k+1)\boldsymbol{A}_t + \boldsymbol{P}_t(k+1)\right]\Delta\boldsymbol{T}\right\} = -(\boldsymbol{F}_n\delta\boldsymbol{n} + \boldsymbol{F}_t\Delta\boldsymbol{T}) \tag{17}$$

and three matrix equations

$$\begin{aligned} \boldsymbol{P}_n(k) &= \boldsymbol{P}_n(k+1) + \boldsymbol{G}_n - \boldsymbol{P}_{nt}(k+1)\boldsymbol{P}_S(k+1)\boldsymbol{P}_{nt}^T(k+1) \\ \boldsymbol{P}_{nt}(k) &= \boldsymbol{P}_{nt}(k+1) + \left[\boldsymbol{P}_n(k+1) - \boldsymbol{P}_{nt}(k+1)\boldsymbol{P}_S(k+1)\boldsymbol{P}_{nt}^T(k+1)\right]\boldsymbol{A}_t \\ &\quad - \boldsymbol{P}_{nt}(k+1)\boldsymbol{P}_S(k+1)\boldsymbol{P}_t(k+1) \\ \boldsymbol{P}_t(k) &= \boldsymbol{P}_t(k+1) + \boldsymbol{P}_{nt}^T(k+1)\boldsymbol{A}_t + \boldsymbol{A}_t^T\boldsymbol{P}_{nt}(k+1) \\ &\quad - \boldsymbol{P}_t(k+1)\boldsymbol{P}_S(k+1)\boldsymbol{P}_{nt}^T(k+1)\boldsymbol{A}_t \\ &\quad - \boldsymbol{P}_t(k+1)\boldsymbol{P}_S(k+1)\boldsymbol{P}_t(k+1) + \boldsymbol{G}_t \end{aligned} \tag{18}$$

where $\boldsymbol{P}_S = (\boldsymbol{G}_V + \boldsymbol{P}_t)^{-1}$.

The corresponding steady-state Riccati equations are

$$\begin{aligned} &\boldsymbol{P}_{nt}\boldsymbol{P}_S\boldsymbol{P}_{nt}^T = \boldsymbol{G}_n, \qquad (\boldsymbol{P}_n - \boldsymbol{G}_n)\boldsymbol{A}_t - \boldsymbol{P}_{nt}\boldsymbol{P}_S\boldsymbol{P}_t = \boldsymbol{0} \\ &\boldsymbol{P}_{nt}^T\boldsymbol{A}_t + \boldsymbol{A}_t^T\boldsymbol{P}_{nt} - \boldsymbol{P}_t\boldsymbol{P}_S\boldsymbol{P}_{nt}^T\boldsymbol{A}_t - \boldsymbol{P}_t\boldsymbol{P}_S\boldsymbol{P}_t + \boldsymbol{G}_t = \boldsymbol{0} \end{aligned} \tag{19}$$

The numerical solutions of these equations for different N are given in the Appendix. An asymptotic solution of the Riccati equation (19) for $\boldsymbol{G}_V \to \boldsymbol{0}$ and $\boldsymbol{G}_t \to \boldsymbol{0}$ is

$$\boldsymbol{P}_n = 2\boldsymbol{G}_n, \qquad \boldsymbol{P}_{nt} = \boldsymbol{G}_n\boldsymbol{A}_t, \qquad \boldsymbol{P}_t = \boldsymbol{A}_t^T\boldsymbol{G}_n\boldsymbol{A}_t \tag{20}$$

In this case, the state vector $\Delta\boldsymbol{T}$ belong to an unstable subspace.

Analytic Solution of Two-Satellite, Linear-Quadratic Formation Keeping

For the simplest satellite constellation from two satellites, the state vector and control vector are $\boldsymbol{x}^T = (\delta n, \Delta T_1, \Delta T_2)$ and $\boldsymbol{v}^T = (\Delta V_1, \Delta V_2)$, respectively. The transposed incidence matrix is $\boldsymbol{A}_t = [-1 \ \ 1]$. Suppose that the weighting matrices are $\boldsymbol{G}_V = \boldsymbol{I}_2$ and $\boldsymbol{G}_X = \mathrm{diag}(g_n, g_t, g_t)$, where $g_n > 0$ and $g_t > 0$. We have $\boldsymbol{P}$ in the form

$$\boldsymbol{P} = \begin{bmatrix} p_n & p_{nt} & -p_{nt} \\ p_{nt} & p_t & p_{tt} \\ -p_{nt} & p_{tt} & p_t \end{bmatrix} \tag{21}$$

Equation (19) yields the four equations. Because this leads to somewhat involved expressions, we give only the outcome:

$$2p_{nt}^2 + g_n\mu = 0 \tag{22a}$$

$$p_n\mu + 2p_{nt}^2 + (p_{tt} - p_t)p_{nt} = 0 \tag{22b}$$

$$\beta + g_t\left(p_{tt}^2 - p_t^2 - p_t - 1\right) + p_n p_{tt}^2 + p_t^3 + p_t^2 = 0 \tag{22c}$$

$$\beta + p_{tt}\left(p_n p_{tt} - p_t^2 - p_t\right) + p_{tt}^3 = 0 \tag{22d}$$

where

$$\mu = p_{tt} - p_t - 1 \tag{23}$$

$$\beta = 2p_{nt}(p_{nt}+1)(p_{tt}+p_t+1) - (p_t+1)^2 p_n \tag{24}$$

First, Eq. (22) gives

$$p_{nt}^2 = -\tfrac{1}{2}(p_{tt} - p_t - 1)g_n \tag{25}$$

Substituting from

$$p_n = g_n + \frac{g_n - 2p_{nt}^2}{2p_{nt}} \tag{26}$$

$$p_t = \left(p_{nt}^2/g_n\right) + c_t \tag{27}$$

where

$$c_t = (g_t/4) + \tfrac{1}{4}\sqrt{g_t^2 + 4g_t} - \tfrac{1}{2} \tag{28}$$

and inserting Eq. (27) into Eq. (22) yields the quartic equation for p_{nt}

$$4p_{nt}^4 + 4g_n p_{nt}^3 - 2(g_t+2)g_n p_{nt}^2 + 2g_n^2 p_{nt} + g_n^2 = 0 \tag{29}$$

After further simplification, we can obtain the following equation:

$$\left\{p_{nt}^2 + [(g_n/2) + 2c_{nt2}]p_{nt} + (g_n/2)\right\} \times \left\{p_{nt}^2 + [(g_n/2) - 2c_{nt2}]p_{nt} + (g_n/2)\right\} = 0 \tag{30}$$

where

$$c_{nt2} = \sqrt{(g_n/2) + (g_n g_t/8) + \left(g_n^2/16\right)} \tag{31}$$

The four roots of Eq. (30) are

$$p_{nt1,2} = -c_{nt2} - (g_n/4) \pm \sqrt{[c_{nt2} + (g_n/4)]^2 - (g_n/2)} \tag{32a}$$

$$p_{nt3,4} = c_{nt2} - (g_n/4) \pm \sqrt{[c_{nt2} - (g_n/4)]^2 - (g_n/2)} \tag{32b}$$

The real root of Eq. (30), which corresponds to the positive definite matrix $\boldsymbol{P}$, is the required solution. The necessary and sufficient conditions of the positive definition are

$$p_t > 0, \qquad p_t^2 - p_{tt}^2 > 0, \qquad \det(\boldsymbol{P}) > 0 \tag{33}$$

These relations are satisfied if

$$p_{nt} > \max(\sqrt{g_n/2}, g_t/2) \qquad \text{or} \qquad p_{nt} < -\sqrt{g_n/2} \tag{34}$$

The root p_{nt2} is always a real negative number in which

$$p_{nt2} < -\sqrt{g_n/2} \tag{35}$$

The state-feedback matrix is

$$\boldsymbol{F} = \begin{bmatrix} f_n & f_{tt} & f_t \\ -f_n & f_t & f_{tt} \end{bmatrix} \tag{36}$$

where

$$f_n = g_n/2p_{nt} \tag{37a}$$

$$f_{tt} = -\frac{\left[(2p_{nt}+1)g_n - 4p_{nt}^2\right]c_{nt2} + (2p_{nt}+1)g_n - 3p_{nt}^2}{4p_{nt}^2(c_{nt2}+1)} \tag{37b}$$

$$f_t = \frac{(c_{nt2}+1)(2p_{nt}+1)g_n - p_{nt}^2}{4p_{nt}^2(c_{nt2}+1)} \tag{37c}$$

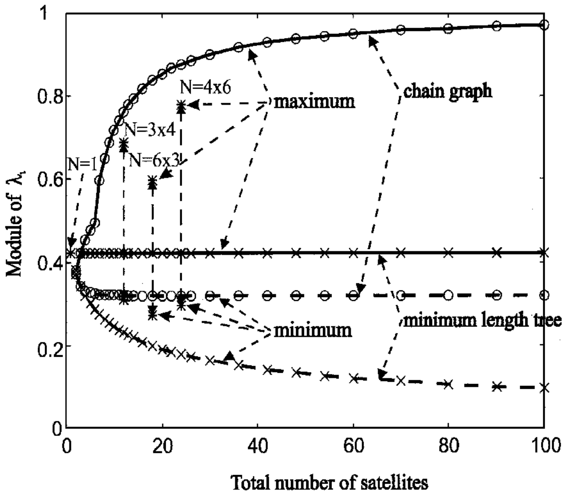

Fig. 4 Minimum and maximum |λ|.

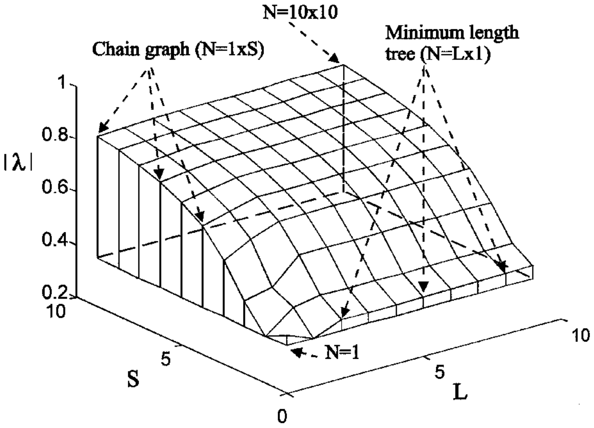

Fig. 5 Maximum |λ| for tree digraphs $L \times S$ (see Fig. 3c).

Stability and Robustness of LQF

The linear system (14) and (15) using the control law (17) is asymptotically stable for an arbitrary total number of satellites. The settling time of the mean square tracking error for different N depends on the closed-loop eigenvalues. It is known that all responses are linear combinations of functions of the form λ^k, $k = 1, 2, \ldots,$ where λ is a closed-loop eigenvalue.[17] An estimate of the 1% settling time of an asymptotically stable discrete-time control systems is[17]

$$k_{1\%} = \max_l\{2/\lg_{10}(1/|\lambda_l|)\}, \qquad l = 1, 2, \ldots, 2N-1 \tag{38}$$

time intervals. The maximum and minimum $|\lambda|$ are shown in Fig. 4. As can be seen, the maximum $|\lambda|$ for the MLT is independent of N and corresponds to $k_{1\%} = 3$. On the other hand, for the CG involving larger values of N, it is close to the stability limit and corresponds to $k_{1\%} = 16$ (for $N = 12$). The maximum $|\lambda|$ depends critically on digraph length. As an example, Fig. 5 shows the maximum $|\lambda|$ for the tree digraph in Fig. 3c.

Because the design is usually based on the nominal values of the mathematical model, it is very important to assess the sensitivity of the system stability to parameter variations. Consider the sensitivity of the LQF to the redistribution of maneuver times. For this estimation we used statistical computations of the closed-loop eigenvalues. The nonzero elements of the submatrix $\boldsymbol{A}_t$ in Eq. (7) have random, uniformly distributed deviations relative to the mean time Δt, i.e., the actual time between maneuvers of each satellite is $\Delta t_i \neq \Delta t$. Typical results (Fig. 6) show that the redistribution of maneuver times Δt_i relative to the mean time Δt retains the stability of the satellite constellation.

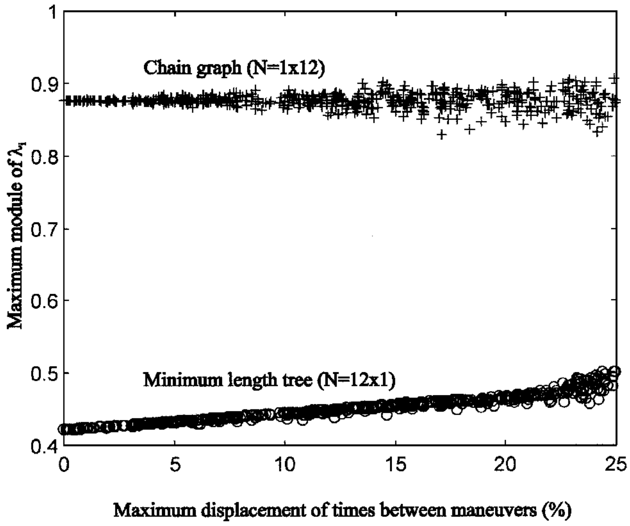

Fig. 6 Statistical estimations of maximum $|\lambda|$, N = 12.

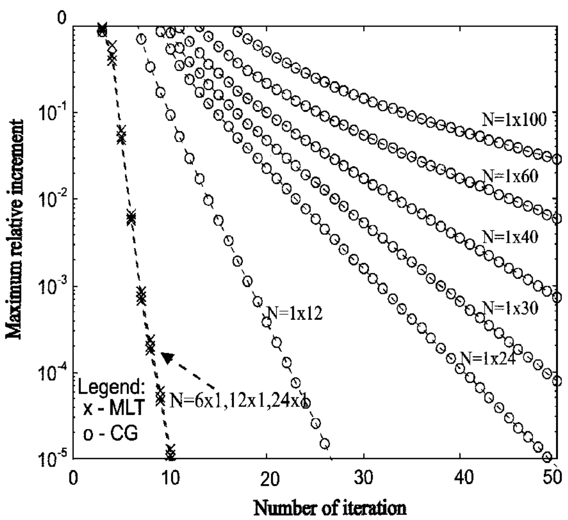

Fig. 7 Maximum relative increments of matrix P for the MLT and the CG.

Solution of Riccati Equation for LQF

There are several ways to obtain a steady-state solution of the Riccati equation.[16,18] A simple method is to start with the non-steady-state Riccati equation (18); begin the solution with terminal conditions [$\boldsymbol{P}_n(0) = \boldsymbol{0}, \boldsymbol{P}_{nt}(0) = \boldsymbol{0}$, and $\boldsymbol{P}_t(0) = \boldsymbol{0}$]; and iterate the equation until a state solution is obtained.[16] It is well known that the convergence rate depends on closed-loop eigenvalues, i.e., digraph length. To illustrate this property, a typical plot of the maximum relative increments for matrix $\boldsymbol{P}$ elements vs the iteration number is shown in Fig. 7. For the MLT, the convergence rate is independent of N. For the CG, it decreased with increasing N.

IV. Simulation Results

To test the performance of the feedback procedure developed in the preceding sections, a code has been written to simulate the dynamics of a low-altitude satellite constellation affected by atmospheric drag. The orbital perturbations of aerodynamic drag will cause the orbits of the individual satellites to decay at different rates, establishing a relative drift between them. The truth orbits are computed by numerically integrating the equations of satellite motion using the Earth's gravitational anomalies and the dynamic atmospheric density model including the diurnal bulge effect.[19] We consider the low-altitude unphased satellite constellation of single continuous coverage of Russia including 5 orbit planes and 12 satellites in each orbit plane.[20] The orbit parameters are altitude of 500 km and inclination of 62.8 deg. The formation keeping of an unphased satellite constellation[21] is similar to the formation keeping of a satellite ring. The impulsive velocity changes ΔV_i are computed using the solution of the steady-state Riccati equation for the MLT (see Appendix). The control law in dimensional form can be written as

$$\boldsymbol{v}(k) = -\frac{0.003797}{\Delta t}\boldsymbol{F}_n \delta\boldsymbol{n} - 0.4415\boldsymbol{F}_t \Delta\boldsymbol{T} \tag{39}$$

where

$$\boldsymbol{F}_n = \begin{bmatrix} f_{n1} & f_{n1} & f_{n1} & f_{n1} & f_{n1} & f_{n1} & f_{n1} & f_{n1} & f_{n1} & f_{n1} & f_{n1} \\ f_{nn} & f_{n2} & f_{n2} & f_{n2} & f_{n2} & f_{n2} & f_{n2} & f_{n2} & f_{n2} & f_{n2} & f_{n2} \\ f_{n2} & f_{nn} & f_{n2} & f_{n2} & f_{n2} & f_{n2} & f_{n2} & f_{n2} & f_{n2} & f_{n2} & f_{n2} \\ f_{n2} & f_{n2} & f_{nn} & f_{n2} & f_{n2} & f_{n2} & f_{n2} & f_{n2} & f_{n2} & f_{n2} & f_{n2} \\ f_{n2} & f_{n2} & f_{n2} & f_{nn} & f_{n2} & f_{n2} & f_{n2} & f_{n2} & f_{n2} & f_{n2} & f_{n2} \\ f_{n2} & f_{n2} & f_{n2} & f_{n2} & f_{nn} & f_{n2} & f_{n2} & f_{n2} & f_{n2} & f_{n2} & f_{n2} \\ f_{n2} & f_{n2} & f_{n2} & f_{n2} & f_{n2} & f_{nn} & f_{n2} & f_{n2} & f_{n2} & f_{n2} & f_{n2} \\ f_{n2} & f_{n2} & f_{n2} & f_{n2} & f_{n2} & f_{n2} & f_{nn} & f_{n2} & f_{n2} & f_{n2} & f_{n2} \\ f_{n2} & f_{n2} & f_{n2} & f_{n2} & f_{n2} & f_{n2} & f_{n2} & f_{nn} & f_{n2} & f_{n2} & f_{n2} \\ f_{n2} & f_{n2} & f_{n2} & f_{n2} & f_{n2} & f_{n2} & f_{n2} & f_{n2} & f_{nn} & f_{n2} & f_{n2} \\ f_{n2} & f_{n2} & f_{n2} & f_{n2} & f_{n2} & f_{n2} & f_{n2} & f_{n2} & f_{n2} & f_{nn} & f_{n2} \\ f_{n2} & f_{n2} & f_{n2} & f_{n2} & f_{n2} & f_{n2} & f_{n2} & f_{n2} & f_{n2} & f_{n2} & f_{nn} \end{bmatrix} \tag{40}$$

$$\boldsymbol{F}_t = \begin{bmatrix} f_{tt}^* & f_{t1} & f_{t1} & f_{t1} & f_{t1} & f_{t1} & f_{t1} & f_{t1} & f_{t1} & f_{t1} & f_{t1} & f_{t1} \\ f_{t3} & f_{tt} & f_{t2} & f_{t2} & f_{t2} & f_{t2} & f_{t2} & f_{t2} & f_{t2} & f_{t2} & f_{t2} & f_{t2} \\ f_{t3} & f_{t2} & f_{tt} & f_{t2} & f_{t2} & f_{t2} & f_{t2} & f_{t2} & f_{t2} & f_{t2} & f_{t2} & f_{t2} \\ f_{t3} & f_{t2} & f_{t2} & f_{tt} & f_{t2} & f_{t2} & f_{t2} & f_{t2} & f_{t2} & f_{t2} & f_{t2} & f_{t2} \\ f_{t3} & f_{t2} & f_{t2} & f_{t2} & f_{tt} & f_{t2} & f_{t2} & f_{t2} & f_{t2} & f_{t2} & f_{t2} & f_{t2} \\ f_{t3} & f_{t2} & f_{t2} & f_{t2} & f_{t2} & f_{tt} & f_{t2} & f_{t2} & f_{t2} & f_{t2} & f_{t2} & f_{t2} \\ f_{t3} & f_{t2} & f_{t2} & f_{t2} & f_{t2} & f_{t2} & f_{tt} & f_{t2} & f_{t2} & f_{t2} & f_{t2} & f_{t2} \\ f_{t3} & f_{t2} & f_{t2} & f_{t2} & f_{t2} & f_{t2} & f_{t2} & f_{tt} & f_{t2} & f_{t2} & f_{t2} & f_{t2} \\ f_{t3} & f_{t2} & f_{t2} & f_{t2} & f_{t2} & f_{t2} & f_{t2} & f_{t2} & f_{tt} & f_{t2} & f_{t2} & f_{t2} \\ f_{t3} & f_{t2} & f_{t2} & f_{t2} & f_{t2} & f_{t2} & f_{t2} & f_{t2} & f_{t2} & f_{tt} & f_{t2} & f_{t2} \\ f_{t3} & f_{t2} & f_{t2} & f_{t2} & f_{t2} & f_{t2} & f_{t2} & f_{t2} & f_{t2} & f_{t2} & f_{tt} & f_{t2} \\ f_{t3} & f_{t2} & f_{t2} & f_{t2} & f_{t2} & f_{t2} & f_{t2} & f_{t2} & f_{t2} & f_{t2} & f_{t2} & f_{tt} \end{bmatrix} \tag{41}$$

Here $\boldsymbol{v}$ is in meters per second, Δt is in days, $\delta\boldsymbol{n}$ is in kilometers, and $\Delta\boldsymbol{T}$ is in seconds. The numerical values of the feedback coefficients are presented in Table 1.

The change in eccentricity due to perturbations causes a daily excursion in along-track displacements that is a significant value. Thus, to minimize the periodic displacements, the eccentricity must be corrected such that the maximum eccentricity during the interval between maneuvers is minimized. Previous robustness analysis is a basis of eccentricity control. The actual maneuver times can be displaced. If $\Delta V_i(k) > 0$, the maneuver must be executed at apogee nearest to the mean time Δt, and if $\Delta V_i(k) < 0$, the maneuver must be executed at perigee (Fig. 8).

The control law depends on the state of all of the satellites and requires computation of the orbital elements. We assume control using a ground segment comprising ground stations and mission control center.

The random perturbations are shorter-term, day-to-day variations of the ballistic coefficients, maneuver errors, and orbit determination errors. All of the perturbations are the normal distributions with mean values and standard deviation (Table 2). Table 3 presents the

Table 1 Feedback coefficients

f_{nn}	f_{n1}	f_{n2}	f_{tt}^*	f_{tt}	f_{t1}	f_{t2}	f_{t3}
−0.3975	0.0420	0.0246	1.2034	1.2066	−0.0609	−0.0373	−0.2651

Table 2 Statistical characteristics of perturbations

Perturbation	Parameter	Mean value	Deviation
Atmospheric drag	Ballistic coefficient, m^2/kg	0.02	0.001
Maneuver errors	$\|\Delta V_i\|$, %	0	2.0
	Orientation errors, deg	0	1.0
Orbit determination	$\|\Delta T_i\|$, s	0	0.005
errors	Δn_i, km	0	5

Table 3 Simulation results

	Solar activity values		
Parameter	Small	Middle	Maximum
Δt, days	13.76	6.88	6.88
Total ΔV per year, m/s			
Mean	0.63	2.94	14.85
Maximum	0.66	2.98	14.98
$\|\Delta V_i\|$, m/s			
Mean	0.023	0.055	0.280
Maximum	0.061	0.107	0.454
$\|\delta n_j\|$, km			
Maximum periodic	19.0	19.0	20.6
Maximum summarized	60.3	36.6	113.1
$\|\Delta T_i\|$, s			
Mean	0.073	0.151	0.860
Maximum	0.216	0.378	1.716
Maximum eccentricity	0.0014	0.0014	0.0015
Total reboost ΔV per year, m/s	0.62	2.86	14.20

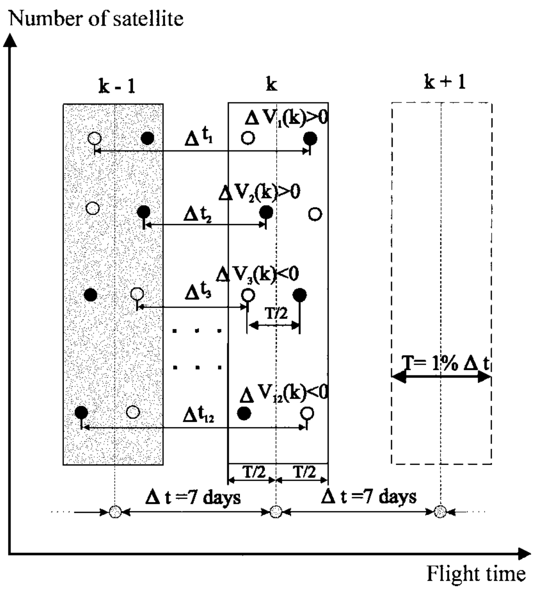

Fig. 8 Schematic representation of maneuver time deviations: ○, apogee; †, perigee; Δt_i, actual time between maneuvers; and Δt, mean time between maneuvers.

simulation results for the LQF and reboost maneuvers required to maintain near-constant altitude of satellite orbit (without formation keeping) for one year.

It is shown that a difference of total ΔV between the LQF and reboost is small. This means additional ΔV for formation keeping of the satellite constellation are approximately 2–7% from reboost ΔV. For small solar activity, we have certain velocity changes $\Delta V_i(k) < 0$ because atmospheric drag is small and the reboost component is comparable with the formation keeping component. For middle and maximum solar activity, the reboost component far exceeds the formation keeping component. This means the formation keeping is realized by small deviations of the reboost components. The general nature of the stochastic processes of the along-track relative displacements δn_i and orbital period displacements ΔT_i for middle solar activity is shown in Figs. 9 and 10, respectively. These parameters are defined not only at maneuver times but also at intermediate times. The velocity changes ΔV_i are shown in Fig. 11. It is

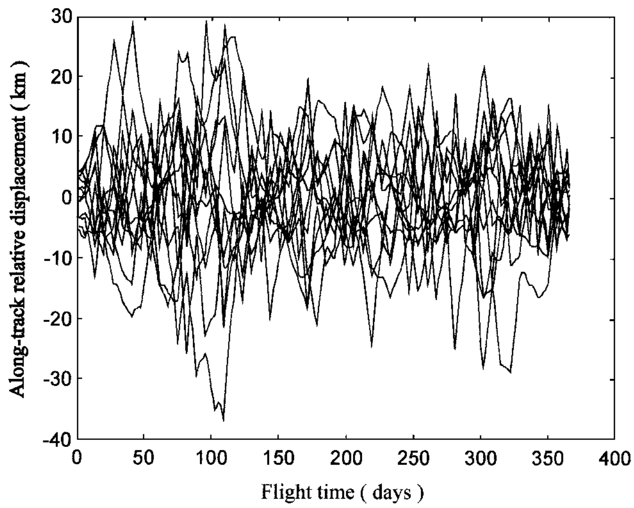

Fig. 9 Time histories of along-track relative displacements.

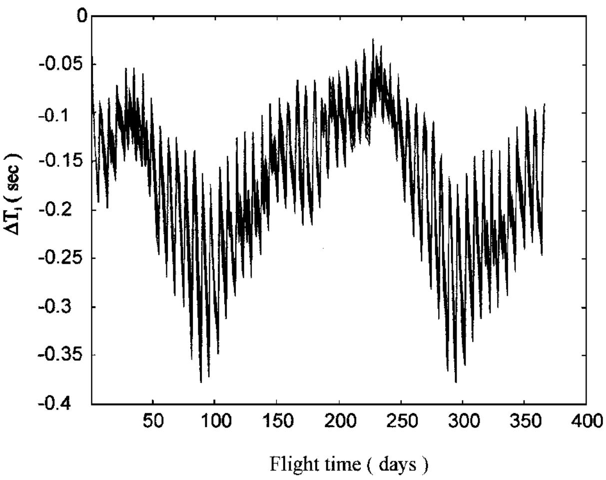

Fig. 10 Time histories of orbital period displacements.

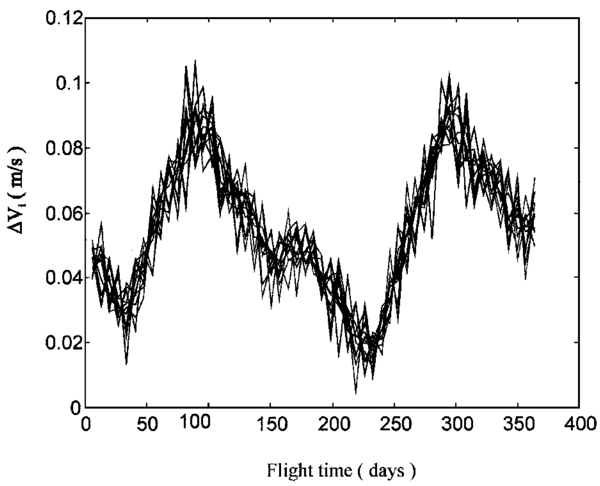

Fig. 11 Time histories of impulsive velocity changes.

seen that there are two maximum velocity changes. This is clarified by half-year variations of atmospheric density.

V. Conclusion

We propose the formation keeping strategy for satellite constellations in circular orbits, which includes the use of a discrete-time linear-quadratic regulator for feedback control. This formation keeping law minimizes the along-track relative displacements between satellites and the orbital period displacements relative to the reference orbit. We have also analyzed the properties of such

Table A1 Solutions of the Riccati equation

N	p_{n1}	p_{n2}	p_{nt11}	p_{nt12}	p_{nt13}	p_{tt}	p_{t1}	p_{td}	p_{t2}
3	2.7413	−0.2058	1.7943	−2.0609	0.3083	6.2171	−2.1294	4.1491	−0.4641
6	2.8467	−0.1005	1.6690	−2.2189	0.1503	12.9898	−1.9869	4.3871	−0.2260
12	2.8975	−0.0497	1.6531	−2.2950	0.0742	26.4043	−1.9182	4.5016	−0.1116
24	2.9224	−0.0247	1.6305	−2.3323	0.0369	53.1703	−1.8845	4.5577	−0.0554
48	2.9348	−0.0123	1.6193	−2.3508	0.0184	106.6714	−1.8677	4.5855	−0.0276
100	2.9412	−0.0059	1.6135	−2.3604	0.0088	222.5738	−1.8591	4.5999	−0.0132
200	2.9442	−0.0029	1.6108	−2.3648	0.0044	445.4553	−1.8551	4.6065	−0.0066
300	2.9452	−0.0020	1.6199	−2.3663	0.0029	668.3351	−1.8538	4.6087	−0.0044

systems. Simulation results validated the formation keeping law. The dynamic model and the controller presented can be used to answer many design questions relating to formation keeping of satellite constellations.

In future work, the possibility of onboard control using intersatellite links needs to be investigated. Perhaps the explicit inclusion of mean atmospheric drag in averaged equations, as in Ref. 3, will help to increase the formation keeping accuracy for the low-altitude satellite constellation affected by atmospheric drag. A comparison between relative and absolute formation keeping may be very useful.

Appendix: Numerical Solutions of the Riccati Equation for LQF

Numerical examples of the steady-state Riccati equation (19) solutions for the MLT are given next. Suppose that weighting coefficients are $g_{nii} = g_{tii} = 1$ and $g_{vii} = 1$; moreover, the first satellite $g_{vll} = N/2$ (in this case total ΔV of all of the satellites are approximately equal). Matrices $\boldsymbol{P}_n$, $\boldsymbol{P}_{nt}$, and $\boldsymbol{P}_t$ are $(N-1)\times(N-1)$, $(N-1)\times N$, and $N\times N$, respectively. For $N \geq 3$ these matrices can be written as

$$\boldsymbol{P}_n = \begin{bmatrix} p_{n1} & p_{n2} & \cdots & p_{n2} \\ p_{n2} & p_{n1} & \cdots & p_{n2} \\ \cdots & \cdots & \cdots & \cdots \\ p_{n2} & p_{n2} & \cdots & p_{n1} \end{bmatrix} \tag{A1}$$

$$\boldsymbol{P}_{nt} = \begin{bmatrix} p_{nt11} & p_{nt12} & p_{nt13} & \cdots & p_{nt13} \\ p_{nt11} & p_{nt13} & p_{nt12} & \cdots & p_{nt13} \\ \cdots & \cdots & \cdots & \cdots & \cdots \\ p_{nt11} & p_{nt13} & p_{nt13} & \cdots & p_{nt13} \\ p_{nt11} & p_{nt13} & p_{nt13} & \cdots & p_{nt12} \end{bmatrix} \tag{A2}$$

$$\boldsymbol{P}_t = \begin{bmatrix} p_{tt} & p_{t1} & p_{t1} & \cdots & p_{t1} \\ p_{t1} & p_{td} & p_{t2} & \cdots & p_{t2} \\ \cdots & \cdots & \cdots & \cdots & \cdots \\ p_{t1} & p_{t2} & p_{t2} & \cdots & p_{t2} \\ p_{t1} & p_{t2} & p_{t2} & \cdots & p_{td} \end{bmatrix} \tag{A3}$$

The elements of these matrices are presented in Table A1.

References

[1]Manuta, L., "Big LEO Revolution," *Satellite Communication*, Vol. 18, No. 3, 1995, pp. 33–40.

[2]Lamy, A., and Pascal, S., "Station Keeping Strategies for Constellations of Satellites," AAS/AIAA International Symposium on Spaceflight Dynamics, Greenbelt, MD, April 1993; also *Advances in the Astronautical Sciences*, Vol. 84, 1993, pp. 819–834.

[3]Glickman, R. E., "TIDE: A Timed-Destination Approach to Constellation Formation-Keeping," AAS/AIAA 4th Spaceflight Mechanics Meeting, Cocoa Beach, FL, Feb. 1994; also *Advances in the Astronautical Sciences*, Vol. 87, Pt. 2, 1994, pp. 725–743.

[4]Calvet, J. L., Bernussou, J., Garcia, J. M., and Kardoudi, G., "An Optimization Method for the Stationkeeping of a Phased Satellite Constellation," *Space Flight Dynamics 1994*, St. Petersburg and Moscow, 1994, pp. 35–38.

[5]McInnes, C. R., "Autonomous Ring Formation for a Planar Constellation of Satellites," *Journal of Guidance, Control, and Dynamics*, Vol. 18, No. 5, 1995, pp. 1215–1217.

[6]Collins, J. T., Dawson, S., and Wertz, J. R., "Autonomous Constellation Maintenance System," *Proceedings of the AIAA/USU Tenth Annual Conference on Small Satellites*, Utah State Univ., Logan, UT, 1996.

[7]Vassar, R. H., and Sherwood, R. B., "Formationkeeping for a Pair of Satellites in a Circular Orbit," *Journal of Guidance, Control, and Dynamics*, Vol. 8, No. 2, 1985, pp. 235–242.

[8]Leonard, C. L., Hollister, W. M., and Bergman, E. V., "Orbital Formationkeeping with Differential Drag," *Journal of Guidance, Control, and Dynamics*, Vol. 12, No. 1, 1989, pp. 108–113.

[9]Redding, D. C., Adams, N. J., and Kubiak, E. T., "Linear Quadratic Stationkeeping for STS Orbiter," *Journal of Guidance, Control, and Dynamics*, Vol. 12, No. 2, 1989, pp. 248–255.

[10]Middour, J. W., "Along Track Formationkeeping for Satellites with Low Eccentricity," *Journal of the Astronautical Sciences*, Vol. 41, No. 1, 1993, pp. 19–33.

[11]Kumar, R. R., and Seywald, H., "Fuel-Optimal Stationkeeping via Differential Inclusions," *Journal of Guidance, Control, and Dynamics*, Vol. 18, No. 5, 1995, pp. 1156–1162.

[12]Hubert, S., and Swale, J., "Stationkeeping of a Constellation of Geostationary Communications Satellites," AIAA Paper 84-2042, Aug. 1984.

[13]Wilde, D., Görlach, T., Yeung, P. S., and Corio, A. J., "Dual Illumination Collocation," *Space Flight Dynamics 1994*, St. Petersburg and Moscow, 1994, pp. 1–6.

[14]Clohessy, W. H., and Wiltshire, R. S., "Terminal Guidance Systems for Satellite Rendezvous," *Journal of the Aerospace Sciences*, Vol. 27, Sept. 1960, pp. 653–658 and 674.

[15]Busacker, R. G., and Saaty, T. L., *Finite Graphs and Networks*, McGraw–Hill, New York, 1965, Chap. 1.

[16]Ogata, K., *Discrete-Time Control Systems*, Prentice–Hall International, Englewood Cliffs, NJ, 1987, Chap. 12.

[17]Kwakernaak, H., and Sivan, R., *Linear Optimal Control Systems*, Wiley-Interscience, New York, 1972, Chap. 6.

[18]Arnold, W. F., and Laub, A. J., "Generalized Eigenproblem Algorithms and Software for Algebraic Riccati Equations," *Proceedings of the IEEE*, Vol. 72, No. 8, 1984, pp. 1746–1754.

[19]"Upper Atmosphere Model for Ballistic Computations," State Standard of Soviet Union, GOST 22721–77, Gosstandard, Moscow, 1977 (in Russian).

[20]Ulybyshev, Y. P., "Design and Study of Satellite Constellations for Continuous Earth's Coverage. Part 1. Low-Altitude Satellite Constellations of Single and Multiple Global and Zonal Coverage. System Catalogues," NPO "Energia," TR P30647-012, Kaliningrad, Moscow Region, Sept. 1992, pp. 1–173 (in Russian).

[21]Ulybyshev, Y. P., "Low-Altitude Satellite Constellations for Orbit Inclinations of Russian Launch Vehicles," *Space Flight Dynamics 1994*, St. Petersburg and Moscow, 1994, pp. 7–17.